Electronic Supplementary Material (ESI) for Soft Matter.
This journal is © The Royal Society of Chemistry 2018

Electronic Supplementary Information

Temperature-dependent structure and dynamics of highly branched poly(*N*-isopropylacrylamide) in aqueous solution

Ateyyah M. AL-Baradi, Stephen Rimmer, Steven R. Carter, Johann P. de Silva, Stephen M. King, Marco Maccarini, Bela Farago, Laurence Noirez, and Mark Geoghegan

HB-PNIPAM synthesis

Table S1. Quantities used for HB-PNIPAM synthesis

NIPAM/ RAFT ratio	NIPAM	RAFT agent	AIBN	dioxane	yield
(25:1)	2.5 g 22.1 mmol	0.229 g 0.882 mmol	0.1450 g 0.894 mmol	8.75 ml	84% 2.424 g
(60:1)	2.5 g 22.1 mmol	0.095 g 0.367 mmol	0.0598 g 0.369 mmol	9.24 ml	88% 2.2903 g
(90:1)	2.5 g 22.1 mmol	0.0636 g 0.246 mmol	0.0398 g 0.245 mmol	8.54 ml	71% 1.8283 g

Table S2. Quantities used to convert *N*-pyrrole dithioate chain end groups to carboxylic acid in HB-PNIPAM

NIPAM/RAFT feed ratio	DMF to dissolve the polymer	4,4’-azobis-(4-cyanopentanoic acid)	DMF to dissolve the acid	yield
(25:1)	123 ml	8.582 g	22 ml	73% 2.121 g
(60:1)	110 ml	7.659 g	20 ml	75% 1.987 g
(90:1)	88 ml	6.097 g	18 ml	79% 2.132 g

NMR analysis

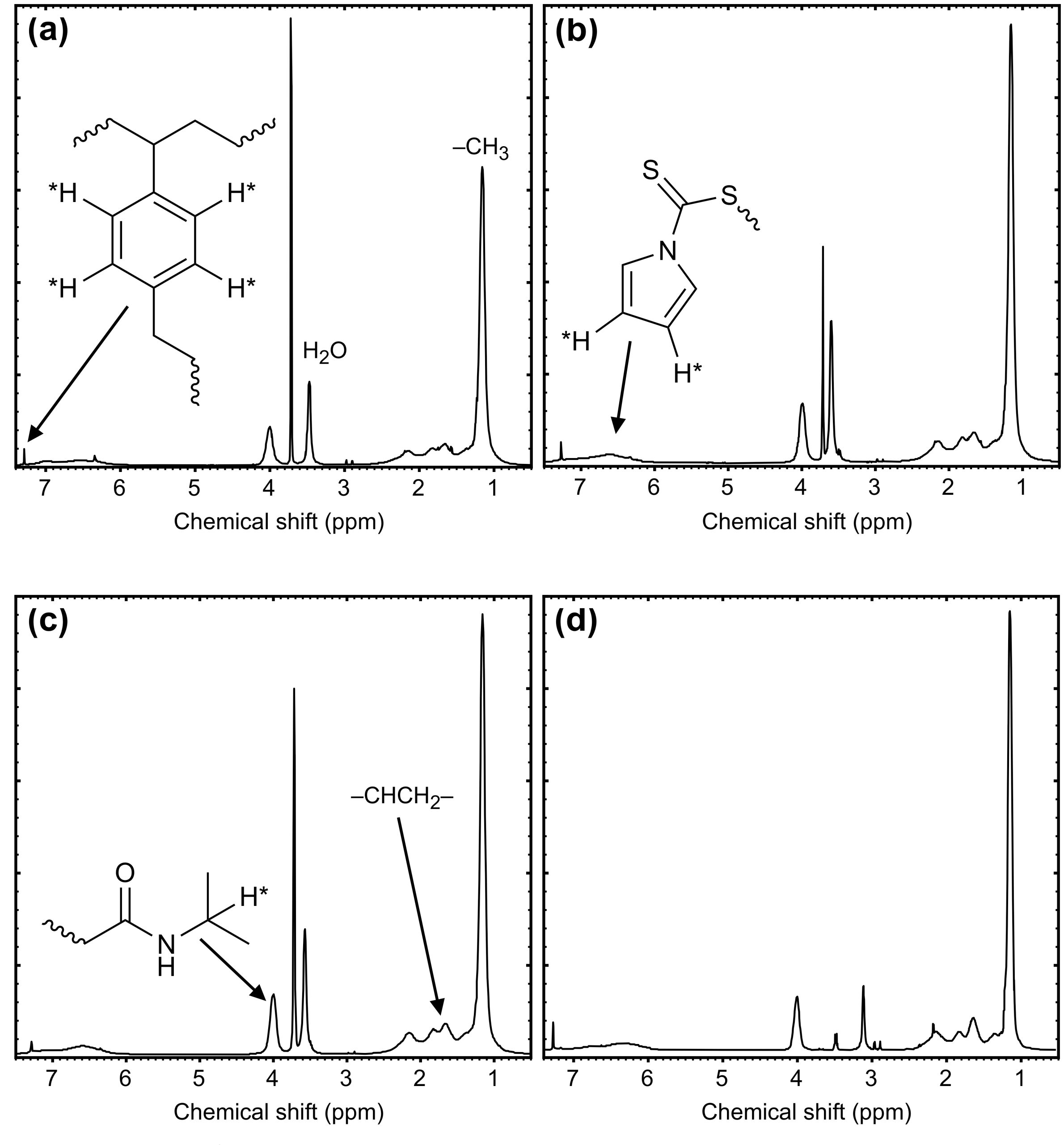

Figure S1. Sample ^1H NMR data for (a) 25:1, (b) 60:1, and (c) 90:1 hyperbranched and (d) linear PNIPAM samples used for SANS experiments. All of the HB-PNIPAM were characterized with NMR to reveal their branching ratios (Table 1 of the main article). Relevant peaks are shown in the figures

Gel permeation chromatography analysis

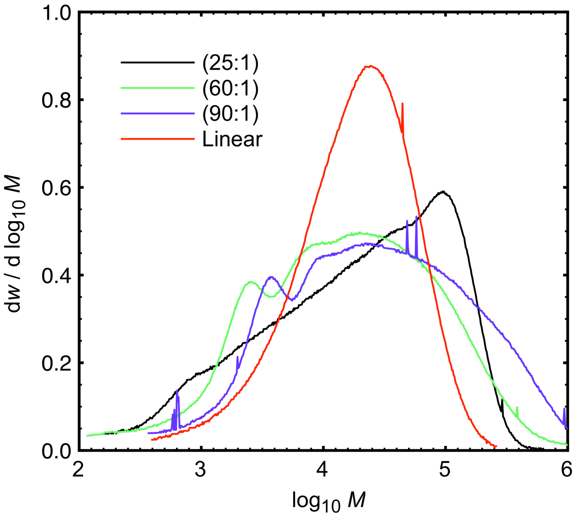

Figure S2. GPC data for HB-PNIPAM used for SANS experiments is shown. The characterization was performed using poly(ethylene glycol) standards and a triple detector with 0.1% tetrabutyl-ammonium bromide as eluent and two PL gel mixed C columns

Rheology

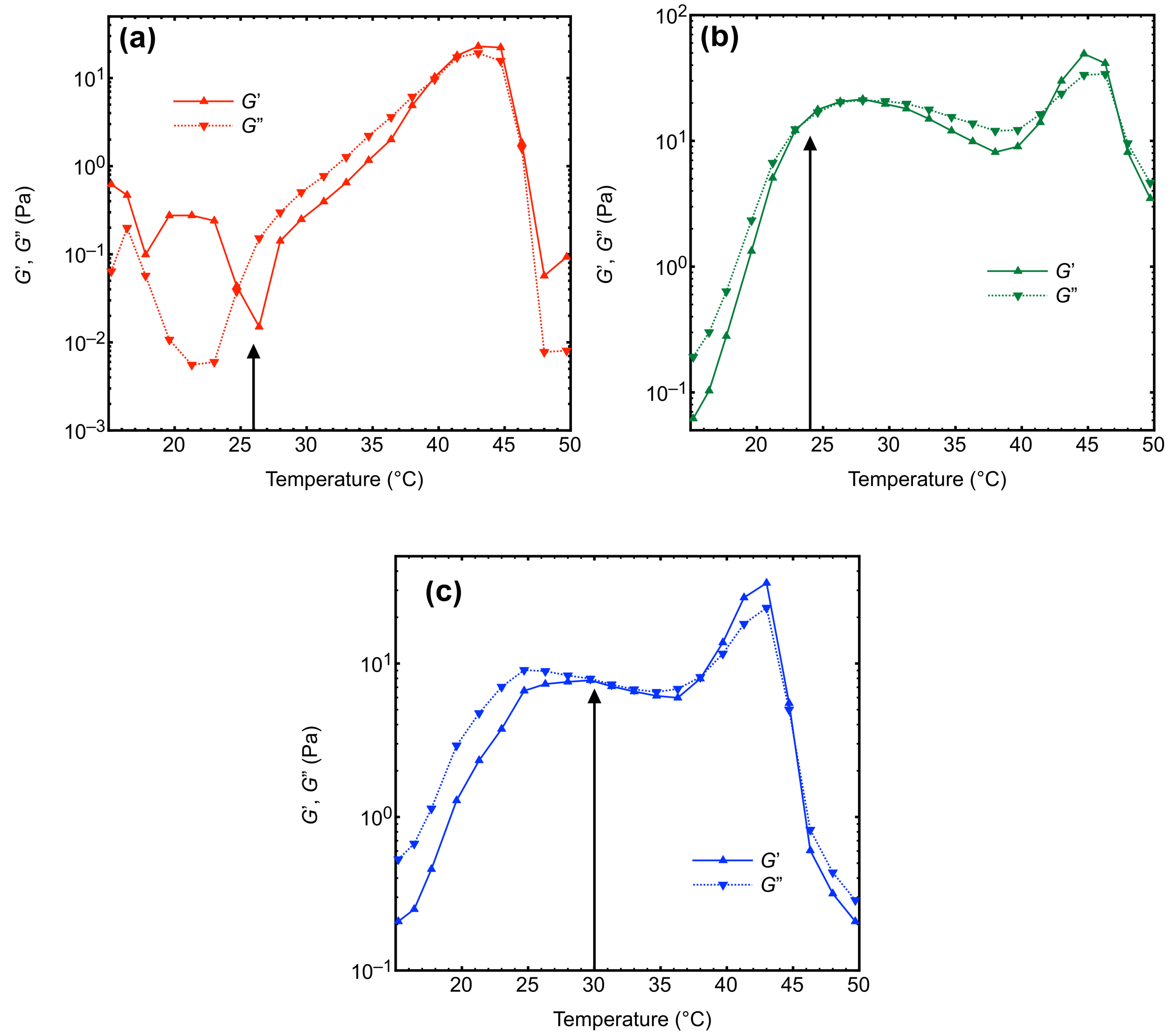

Figure S3. Rheology data for HB-PNIPAM at a concentration in water of 3% with branching ratios (a) 25:1, (b) 60:1, and (c) 90:1. The arrows indicate the LCST for the corresponding 5% samples, which shows that the points of overlap of the storage (*G*') and loss (*G*") moduli are very close to the LCST in each case. These rheological measurements were conducted using an ARES-G2 rheometer with 50 mm diameter plates and a gap of 1 mm. An oscillatory shear at 0.01 Pa was applied at a frequency of 0.5 Hz. The time taken for each measurement was 20 s

SANS results

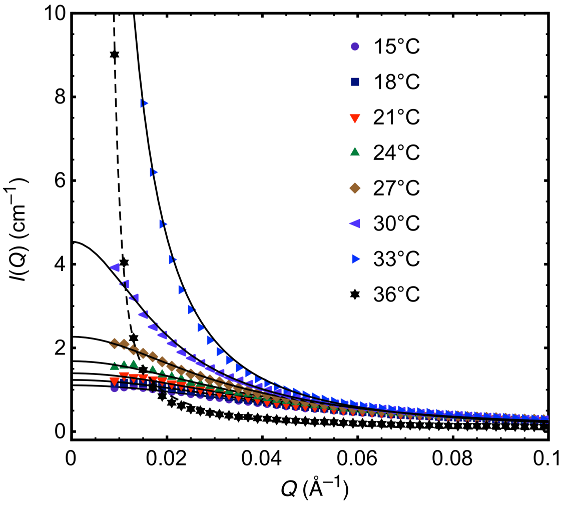

Figure S4. SANS intensity profiles of 5 wt% linear PNIPAM in D_2O as a function of temperature. The data were fitted to eqn 1 below the LCST (solid lines) and the combined Porod-Lorentzian scattering function (eqn 2) above the LCST (broken line). These data and fits are shown with background subtracted and eqns 1 and 2 refer to those in the main article

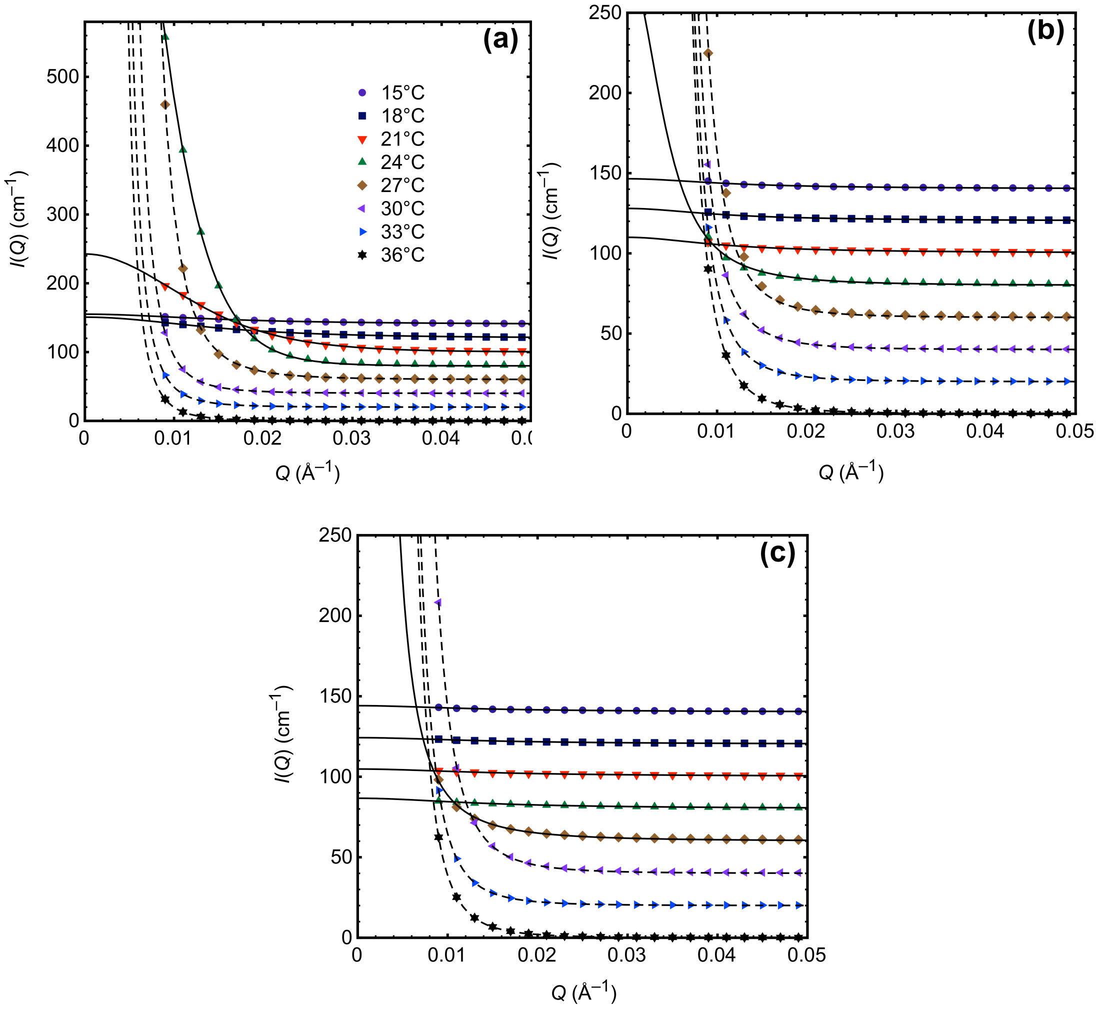

Figure S5. SANS intensity profiles of (a) (25:1), (b), (60:1), and (c) (90:1) 5 wt% HB-PNIPAM in D_2O as a function of temperature. The solid lines, below the LCST, are fits to eqn 1 (main article), and the broken lines, corresponding to data for samples held above the LCST, are fits to a Porod scattering behavior (eqn 2 in the main article with $I_L = 0$). The data have been staggered in multiples of 20 cm^{-1} for clarity. Each curve tends to $I(Q) = 0$ at large Q. These data and fits are shown with background subtracted in Figure 1 (main article)

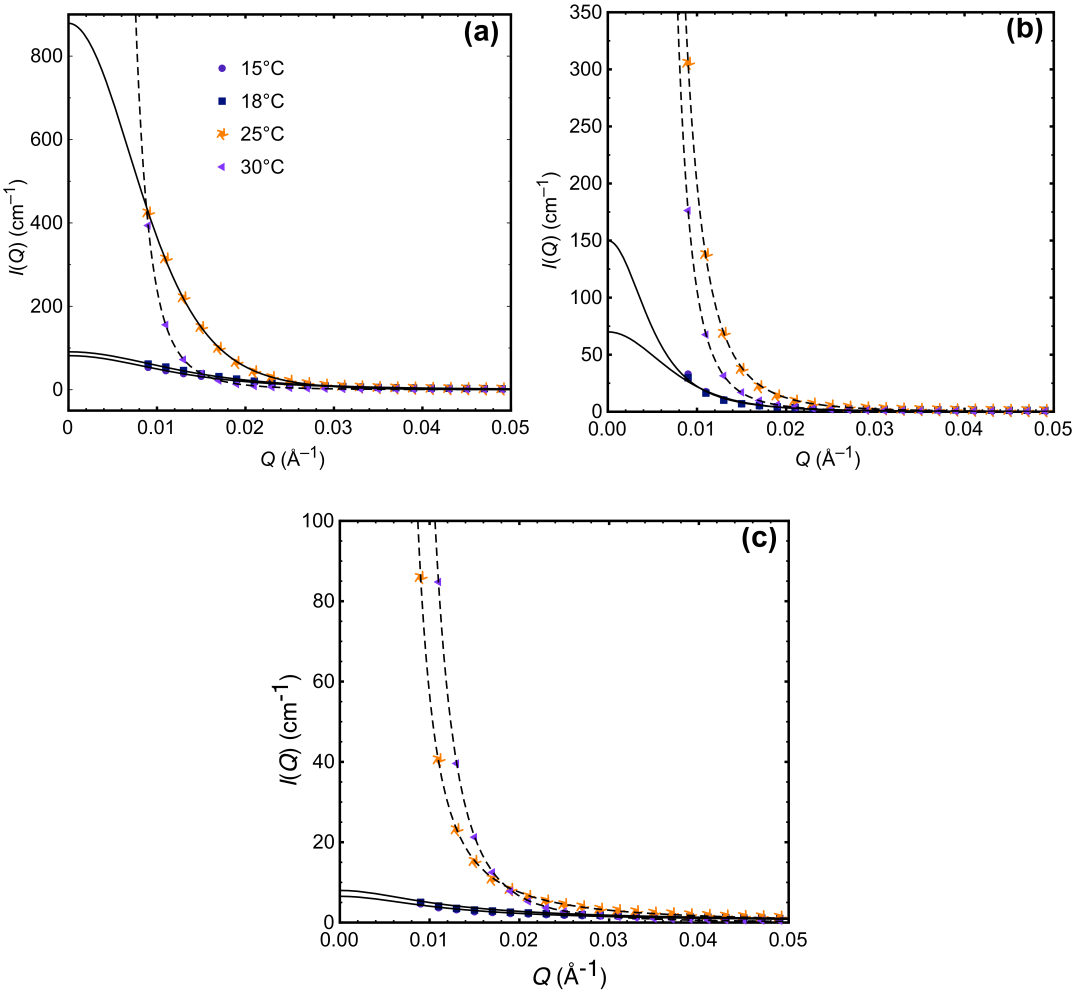

Figure S6. SANS intensity profiles of (a) (25:1), (b) (60:1), and (c) (90:1) 9 wt% HB-PNIPAM as a function of temperature. The solid lines, below the LCST, are fits to eqn (1) (main article), and the broken lines, corresponding to data for samples held above the LCST, are fits to a Porod scattering behavior (eqn 2 in the main article set with $I_L = 0$)

Neutron spin echo results

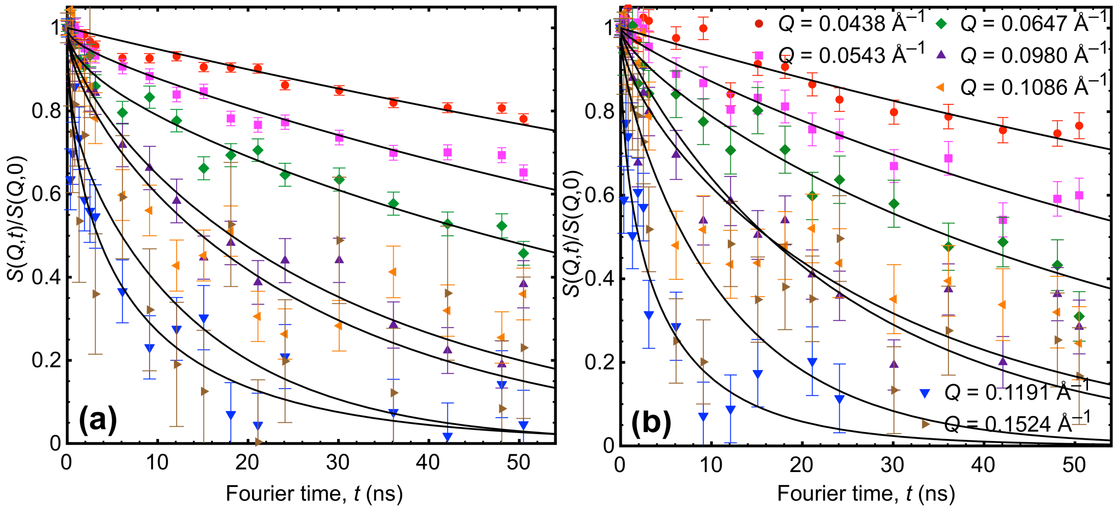

Figure S7. Intermediate scattering function for D7-HB-PNIPAM (a) (25:1) at 25.4°C and (b) (90:1) at 31.1°C in D_2O at the values of Q indicated. The LCST of these polymers at 4% (w/w) concentration is 28°C and 30°C (Table 3). The solid lines are fits to eqn 4 (main article) with $\beta = 1/2$

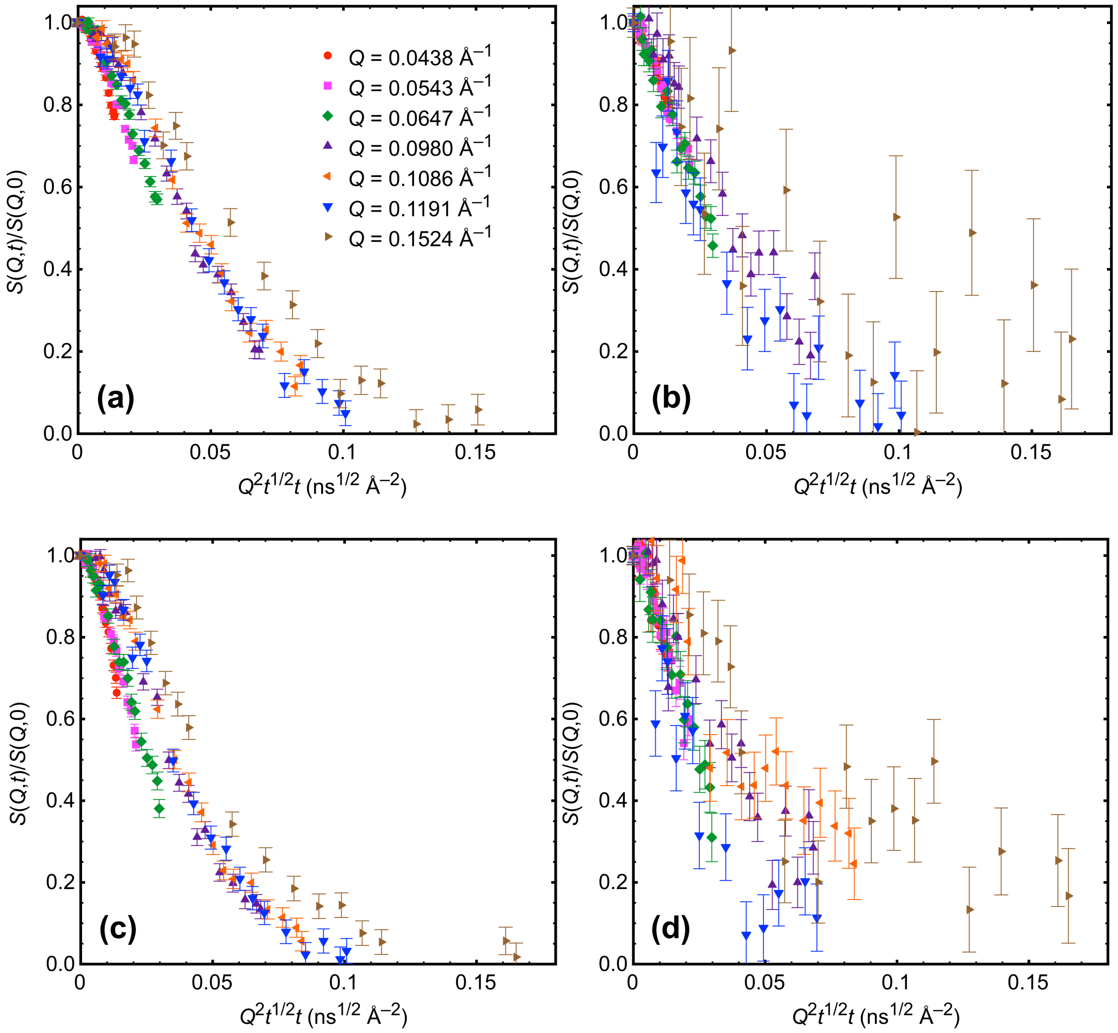

Figure S8. Intermediate scattering function plotted as a function of $Q^2t^{1/2}$ for D**7**-HB-PNIPAM (25:1) at (a) 15°C and (b) 25.4°C and (90:1) at (c) 24°C and (d) 31.1°C in D_2O at the values of Q indicated. If translational diffusion were not a contributing factor, and Rouse internal dynamics were to dominate, the data would be expected to collapse onto a master curve

Table S3a. Fitting results of D7-HB-PNIPAM (25:1) at 15°C (Figure 5a, main article)

Q (Å^{-1})	A	D_0 (10^{-11} m^2/s)	Γ (ns^{-1})
0.0438	1	2.66±0.04	
0.0543	0.990±0.004	2.66	0.5±1.2
0.0647	0.95±0.07	2.66	0.02±0.07
0.0980	0	2.66	0.0015±0.0002
0.1086	0	2.66	0.0027±0.0003
0.1191	0	2.66	0.010±0.001
0.1524	0	2.66	0.014±0.002

Table S3b. Fitting results of D7-HB-PNIPAM (25:1) at 25.4°C (Figure S8a)

Q (Å^{-1})	A	D_0 (10^{-11} m^2/s)	Γ (ns^{-1})
0.0438	1	2.74±0.07	
0.0543	0.94±0.01	2.74	0.3±0.4
0.0647	0.85±0.03	2.74	0.2±0.2
0.0980	0.7±0.2	2.74	0.04±0.09
0.1086	0.8±0.1	2.74	0.1±0.2
0.1191	0.1±0.2	2.74	0.1±0.1
0.1524	0.7±0.1	2.74	1±3

Table S3c. Fitting results of D7-HB-PNIPAM (90:1) at 24.0°C (Figure 5b, main article)

Q (Å^{-1})	A	D_0 (10^{-11} m^2/s)	Γ (ns^{-1})
0.0438	1	3.83±0.08	
0.0543	0.95±0.04	3.83	0.04±0.1
0.0647	0.88±0.04	3.83	0.07±0.08
0.0980	0	3.83	0.0022±0.0003
0.1086	0	3.83	0.0047±0.0006
0.1191	0	3.83	0.013±0.002
0.1524	0	3.83	0.018±0.003

Table S3d. Fitting results of D7-HB-PNIPAM (90:1) at 31.1°C (Figure S8b)

Q (Å^{-1})	A	D_0 (10^{-11} m^2/s)	Γ (ns^{-1})
0.0438	1	3.3±0.2	
0.0543	0	3.32	0.00015±0.00008
0.0647	0	3.32	0.0010±0.0003
0.0980	0.81±0.08	3.32	0.3±0.4
0.1086	0.9±0.1	3.32	0.2±1.6
0.1191	0	3.32	0.18±0.03
0.1524	0.8±0.2	3.32	0.7±2.7

In Table S3 the results for the fitting to eqn 4 in the main article are presented assuming that the internal dynamical term is due to Rouse behavior ($\beta = 1/2$). It is clear that those data closer to the LCST of the D7-HB-PNIPAM (i.e. those results listed in Tables S3b and S3d) are unreliable, with excessive uncertainties associated with the results. The values in the cells shaded in yellow were fixed during the fitting

Confocal laser-scanning microscopy images

The RAFT polymerization procedure described in section 7.2.2 was also used to synthesize linear and hyperbranched PNIPAM with a chemically attached fluorescein to the polymer backbone. The same quantities shown in Table S1 were used were used to prepare fluorescently labeled linear and hyperbranched PNIPAMs, but with the addition of 25 mg (i.e. 1% of the NIPAM quantity) of fluorescein *o*-acrylate (97% from Sigma-Aldrich). The *N*-pyrroledithioate chain-end groups were also converted to carboxylic-acid chain-end groups using the same quantities as in Table S2.

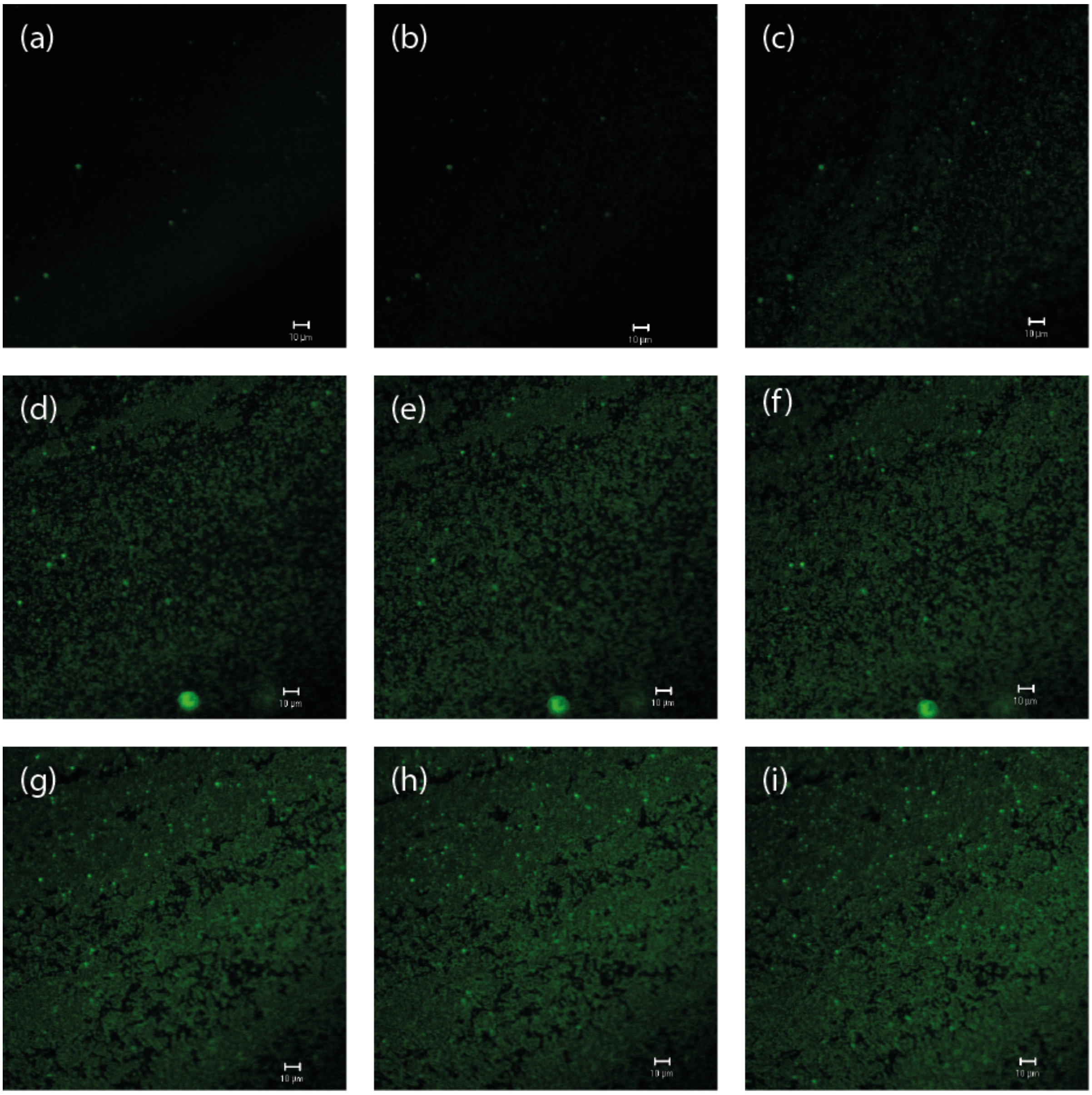

Figure S9. Confocal laser-scanning microscopy images of 5 wt% of HB-PNIPAM (25:1). The temperature range is as follows: (a) 10°C (b) 15°C, (c) 18°C, (d) 21°C, (e) 24°C, (f) 27°C, (g) 30°C, (h) 33°C and (i) 36°C. The polymer swells below the LCST (26°C) and collapses above it, indicated by the increase in aggregate density with temperature. The scale bar in all images is 10 µm

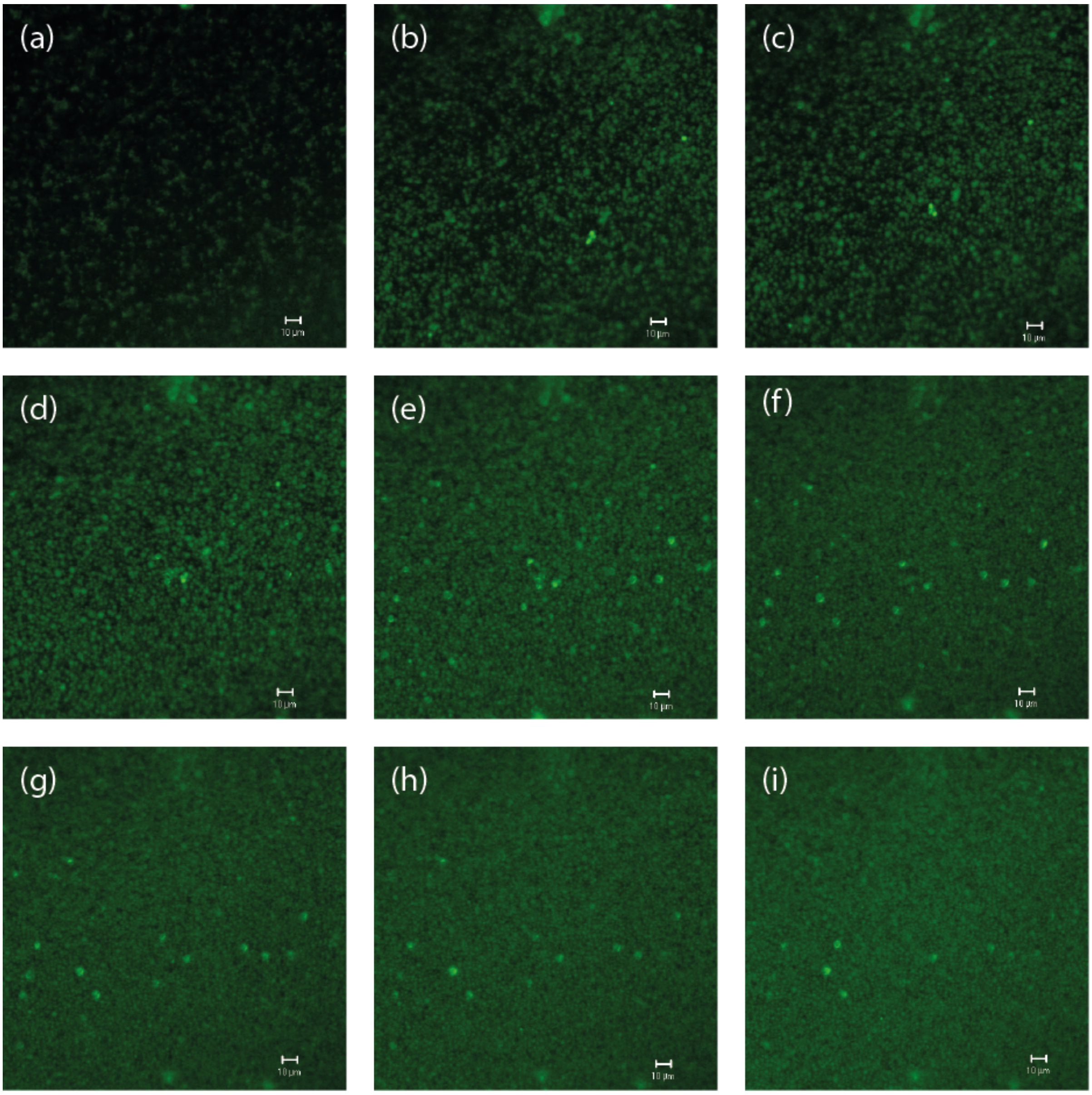

Figure S10. Confocal laser-scanning microscopy images of 5 wt% of HB-PNIPAM (60:1). The temperature range is as follows: (a) 10°C (b) 15°C, (c) 18°C, (d) 21°C, (e) 24°C, (f) 27°C, (g) 30°C, (h) 33°C and (i) 36°C. The polymer swells below the LCST (24°C) and collapses above it, indicated by the increase in aggregate density with temperature. The scale bar in all images is 10 µm

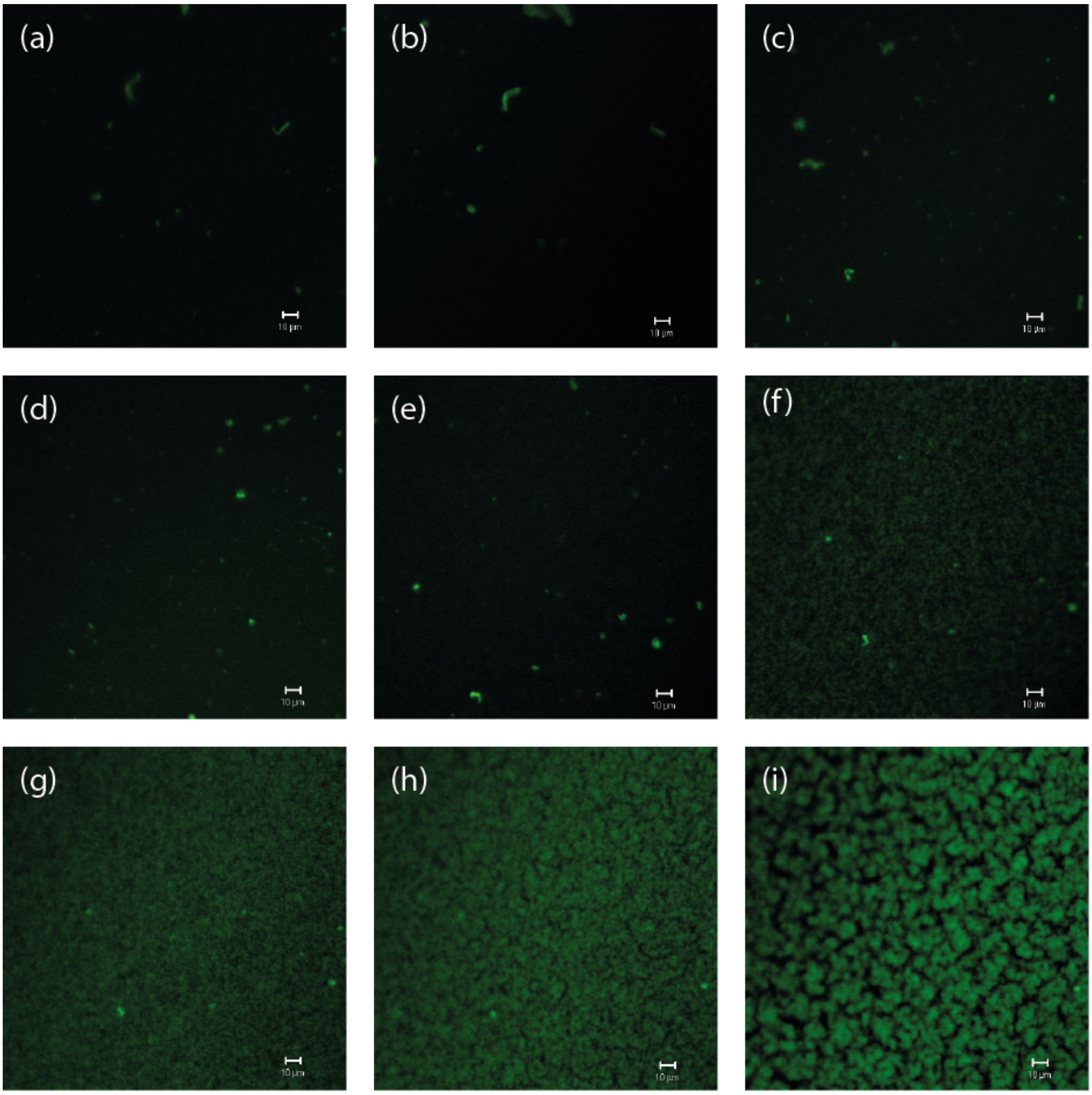

Figure S11. Confocal laser-scanning microscopy images of 5 wt% of HB-PNIPAM (90:1). The temperature range is as follows: (a) 10°C (b) 15°C, (c) 18°C, (d) 21°C, (e) 24°C, (f) 27°C, (g) 30°C, (h) 33°C and (i) 36°C. The polymer swells below the LCST (30°C) and collapses above it, indicated by the increase in aggregate density with temperature. The scale bar in all images is 10 µm

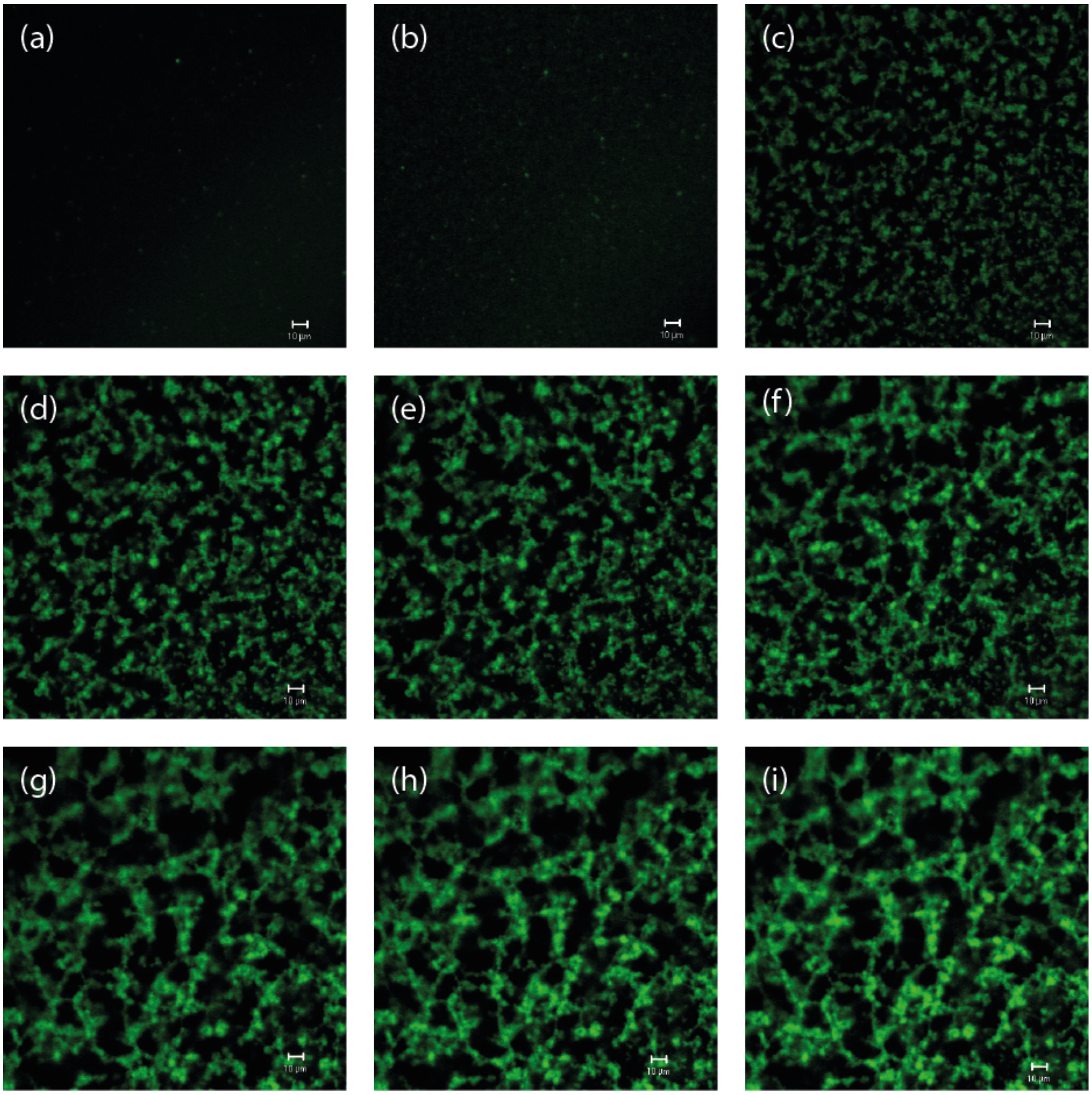

Figure S12. Confocal laser-scanning microscopy images of 5 wt% of linear PNIPAM. The temperature range is as follows: (a) 10°C (b) 15°C, (c) 18°C, (d) 21°C, (e) 24°C, (f) 27°C, (g) 30°C, (h) 33°C and (i) 36°C. The polymer swells below the LCST (32°C) and collapses above it, indicated by the increase in aggregate density with temperature. The structure of the linear polymer aggregates above the LCST has a network topology in contrast to the more uniform distribution of the highly branched polymers. The scale bar in all images is 10 µm